A Study of Transient Radiation from the Wu–King Resistive Monopole—FDTD Analysis and Experimental Measurements

James G. Maloney, *Member, IEEE,* and Glenn S. Smith, *Fellow, IEEE*

Abstract—**The cylindrical monopole antenna with a continuous resistive loading is considered as a radiator for temporally short, broad-bandwidth pulses. Specifically, the variation of the resistance used along the monopole is one proposed by Wu and King (Wu–King profile). This antenna is analyzed by the finite-difference time-domain (FDTD) method utilizing a new, efficient technique for handling the thin-walled, conducting tube that forms the resistance. The electromagnetic field in the space surrounding the antenna is determined as a function of time, and quantities useful for describing the performance of the antenna are then calculated from these results: the reflected voltage in the transmission line, the surface charge density on the antenna, and the time-varying field in the far zone. Graphical displays of these results are used to give new insight into the physical processes for transient radiation from this antenna. An experimental model is constructed using a discretized version of the Wu–King profile formed from a set of precision, high-frequency resistors. The fine details of these resistors are accurately included in the FDTD analysis. Measurements of both the reflected voltage in the feed line and the time-varying radiated field are in excellent agreement with the theoretical calculations.**

I. INTRODUCTION

ANTENNAS that are used to radiate temporally short, broad-bandwidth pulses often have internal reflections, for example, at the drive point and the open end of a dipole antenna [1]. The radiated waveform is then composed of several elements, each of which can be associated with an internal reflection. The unwanted reflections can sometimes be reduced and the shape of the radiated waveform improved by including resistive material in the antenna structure.

Apparently, Altshuler was the first to use resistive loading to reduce reflections on an antenna [2]. He placed discrete resistors a quarter wavelength from the open ends of a dipole to produce an outward-traveling wave on the remainder of the antenna. This approach only works well over a narrow range of frequencies, because of the requirement that the resistors be roughly a quarter wavelength from the open ends. In 1965 Wu and King considered the dipole antenna with continuous resistive loading [3]. They obtained a profile for the loading that produced an outward-traveling wave on the antenna over a broad range of frequencies. This antenna is sometimes referred to as the Wu–King dipole, and the profile for the resistive loading as the Wu–King profile.

Since 1965 many researchers have investigated resistively loaded antennas with the Wu–King profile or a generalization of it [4]. Expressions for the current on the antenna, obtained both analytically and numerically, have been used to compute quantities such as the input impedance and far-field patterns for both linear and vee dipoles [5]–[10]. Experimental models have been constructed using thin coatings of paint or metal alloys with variable thickness deposited on plastic or glass rods [9], [11], [12]. Measurements made on these models have generally been in good qualitative agreement with the theoretical calculations; however, precise agreement was seldom obtained, particularly for the input impedance/admittance of the antenna. The lack of precise agreement results from several factors: the approximations made in the theoretical model and its solution, and the difficulties associated with the fabrication and characterization of the experimental models.

The Wu–King profile has been used with probes, both linear and vee dipoles (monopoles), designed to measure transient electromagnetic fields [13]–[15]. It has also been used with resistive monopole antennas designed for spread-spectrum signaling in wideband HF communication systems [16].

Recently, we have used the finite-difference time-domain (FDTD) method to accurately analyze the transient radiation from perfectly conducting cylindrical and conical monopole antennas [1]. In this paper, we will apply the FDTD method to the Wu–King monopole and present new experimental measurements for this antenna. There are three objectives for this paper: first, to show how the FDTD method can be applied to this type of structure, i.e., one that contains thin sheets of resistive material; second, to present new experimental results made on a well-characterized model of the Wu–King monopole (a discretized version of the profile) and to show that they are in excellent agreement with the FDTD theoretical results; and third, to use graphical displays obtained from the FDTD results to give new insight into the physical processes for transient radiation from this antenna.

II. FORMULATION OF THE ANTENNA PROBLEM AND FDTD ANALYSIS

Fig. 1 shows the cylindrical monopole driven through an image plane by a coaxial transmission line. The conductors of

---

Manuscript received May 15, 1992. This work was supported by the Joint Services Electronics Program under contracts DAAL03-87-K-0059, DAAL-03-90-C-0004, and DAAL-03-89-G-0078 and by a contract between the Army Research Office and the University of Minnesota for the Army High Performance Computing Research Center. Support was also provided by the Joint Services Electronics Program (JSEP) and the DuPont Corporation in the form of a JSEP Graduate Fellowship and a Dupont Fellowship to J. G. Maloney.

The authors are with the School of Electrical Engineering, Georgia Institute of Technology, Atlanta, GA 30332-0250.

IEEE Log Number 9209214.

0018–926X/93$03.00 © 1993 IEEE

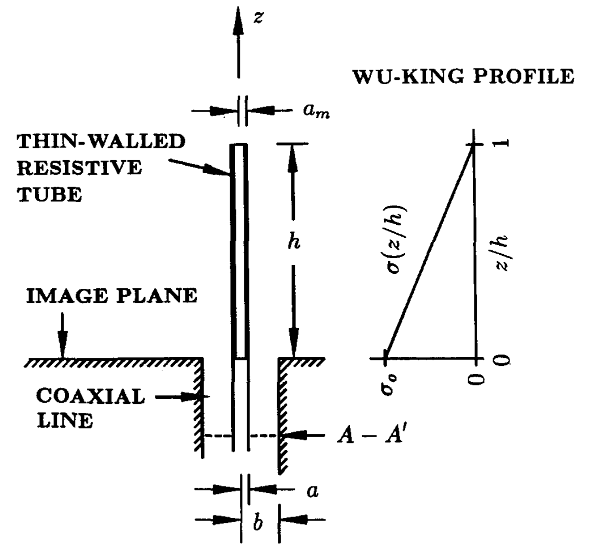

Fig. 1. Geometry for resistive monopole antenna fed through an image plane by a coaxial transmission line.

the coaxial line and the image plane are assumed to be perfect, while the monopole is formed from a thin-walled resistive tube. Following Wu and King, the internal impedance per unit length of this tube will be chosen so as to produce an outward-traveling wave along the monopole.

The internal impedance per unit length for the Wu–King profile is [3]

$$z^i(z/h) = \frac{\zeta_0 \psi}{2\pi h(1 - z/h)}. \tag{1}$$

Here, z/h is the relative distance along the monopole from the coaxial aperture, $\zeta_0 = \sqrt{\mu_0/\epsilon_0}$, and ψ is a dimensionless parameter that is determined from the distribution of current on the antenna. The parameter ψ (a complex number) is a function of h/a_m, the ratio of the height of the monopole to its radius, and $k_0 h = \omega h/c$, the electrical length of the monopole at the frequency ω. Numerical calculations for practical antennas show that ψ exhibits weak frequency dependence, at least at low frequencies, typical low-frequency values for reasonable h/a_m being $6.0 \leq |\psi| \leq 12.0$.

For practical antennas, the complex internal impedance of (1) is usually approximated by a purely resistive internal impedance per unit length:

$$r^i(z/h) = \frac{\zeta_0 \psi_0}{2\pi h(1 - z/h)}, \tag{2}$$

where ψ_0 (a real number) is the zero-frequency value of ψ. If this resistance is obtained using a thin-walled metallic tube of outer radius a_m and wall thickness $d(d \ll a_m)$, as in Fig. 1, the conductivity of the tube must vary with z/h as

$$\sigma(z/h) = (1 - z/h)\sigma_0, \tag{3}$$

where

$$\sigma_0 = \frac{(h/a_m)}{2\pi d \zeta_0 \psi_0}. \tag{4}$$

This profile for the conductivity is shown schematically on the right-hand side of Fig. 1.

The input impedance of the Wu–King monopole is approximately [3]

$$Z = \frac{\zeta_0 \psi}{4\pi}(1 - j/k_0 h). \tag{5}$$

To estimate this impedance, we assume $k_0 h \gg 1$ to obtain

$$Z = \frac{\zeta_0 \psi_0}{4\pi}. \tag{6}$$

For a typical value $\psi_0 = 10$, the input impedance for the monopole is very high, $Z \approx 300\ \Omega$. To minimize reflections at the drive point, the antenna should be driven from a coaxial line that has a characteristic impedance, Z_0, roughly equal to this input impedance. However, this would require a ratio of outer to inner conductor radii $b/a \approx 148$, a very impractical value. For a typical characteristic impedance, $Z_0 = 50\ \Omega(b/a = 2.30)$, the reflection coefficient for this antenna is $\Gamma \approx 0.7$. Thus, we see that a significant reflection will occur at the drive point of the Wu–King monopole when practical parameters are used for the antenna and coaxial feed line. For the dipole fed from a two-wire line, the high input impedance is not a problem.

The formulation of the theoretical model for the resistive monopole antenna and its solution by the FDTD method are essentially the same as presented in the earlier paper for the perfectly conducting antennas [1]; therefore, only the basic features and new additions to the formulation will be described here. On the plane A–A' in the coaxial line shown in Fig. 1, the time-varying, incident electric field is

$$\vec{\mathcal{E}}^i(t) = \frac{\mathcal{V}^i(t)}{r \ln(b/a)}\hat{r}; \tag{7}$$

this is the excitation for the problem. The space surrounding the monopole and extending into the coaxial line to the plane A–A' is discretized, and the three relevant field components ($\mathcal{E}_r$, $\mathcal{E}_z$, $\mathcal{H}_\phi$) are evaluated at the appropriate nodes of the grid. These field components are updated in time using the discretized form of Maxwell's equations [1, eqs. (3a)–(3c)]. The outer boundary of the region surrounding the monopole is placed sufficiently far away that its effect can be gated out in time. The resistive portion of the antenna, the thin-walled tube shown in Fig. 1, is modeled using a new, efficient technique for incorporating thin material sheets into the FDTD method [17].

The FDTD method is used to calculate the electromagnetic field in the space surrounding the antenna as a function of time [18]. The quantities useful for describing the performance of the antenna are then determined from these results: the reflected voltage in the transmission line, the surface charge density on the structure, and the time-varying electric field in the far zone. The field in the far zone is calculated by transforming the near-zone field obtained on a closed surface surrounding the antenna. Methods for performing this transformation are described in [1] and [19].

III. PHYSICAL DESCRIPTION OF THE RADIATION PROCESS

For all examples in this section, the normalized physical dimensions for the antenna are $b/a = 2.30$ ($Z_0 = 50\ \Omega$) and $h/a_m = 65.8$ ($a_m = a$). The parameters for the thin-walled resistive tube used with the Wu–King profile (3), (4) are $\psi_0 = 7.79$, or $\sigma_0 d\zeta_0 = 1.34$. The physical dimensions of the resistive monopole are the same as those used for the perfectly conducting monopole in the earlier paper [1]. This allows a meaningful comparison of the results for the resistive and the perfectly conducting monopoles.

The resistive monopole will be studied first for a Gaussian pulse excitation, the incident electric field being (7) with

$$\mathcal{V}^i(t) = V_0 \exp\left(-t^2/2\tau_p^2\right). \tag{8}$$

The antenna is characterized by the time $\tau_a = h/c$; this is the time required for light to travel its length. The ratio of the characteristic time for the Gaussian pulse, τ_p, to the characteristic time for the antenna, τ_a, is taken to be $\tau_p/\tau_a = 8.04 \times 10^{-2}$.

Fig. 2 shows the "equivalent" surface charge density[1] on the center conductor of the coaxial line and the monopole as a function of the normalized position z/h and the normalized time t/τ_a. This bounce diagram shows that the pulse travels up the line until it reaches the aperture ($z/h = 0.0$, $t/\tau_a = 1.0$; A in Fig. 2). At this point a portion of the pulse is reflected back into the line and a portion emerges onto the monopole. As the pulse travels out along the resistive monopole, it decreases in amplitude while depositing charge along the structure. The decrease in amplitude is roughly linear, as is the profile for the conductivity (3). Notice that there is no distinct reflection at the end of the resistive monopole ($z/h = 1.0$, $t/\tau_a \approx 2.0$). This is to be contrasted with the pulse propagating on the perfectly conducting monopole [1, fig. 4], whose amplitude remains roughly constant while propagating along the structure between reflections at the end and coaxial aperture.

Notice that the charge deposited on the resistive monopole by the initial pulse (B in Fig. 2) slowly drains off the monopole by passing through the coaxial line. For the perfectly conducting monopole, a small amount of charge leaves the monopole by entering the coaxial line each time a pulse reflected from the end is incident on the aperture.

The electric field surrounding the monopole is displayed on a gray scale in Fig. 3 for three times. Graphs of the surface charge density are below each plot; these correspond to the slices marked a, b, and c in Fig. 2. The spacing between the conductors of the coaxial line is expanded in these plots to clarify the presentation.

In Fig. 3(a) a portion of the incident pulse has been reflected at the aperture and the remainder has traveled out onto the monopole. A spherical wavefront centered on the aperture (W_1 in Fig. 3(a)) is attached to packets of charge on the monopole and the image plane. Notice that charge is deposited along the entire length of the monopole as this wavefront, W_1, moves out. This wavefront passes the end of the monopole (Fig. 3(b)) without significant reflection; thus no secondary wavefront is generated at this point. This is to be compared with the results for the perfectly conducting monopole [1, fig. 5(b)], where the reflection of W_1 produces a spherical wavefront, W_2, centered on the end of the monopole.

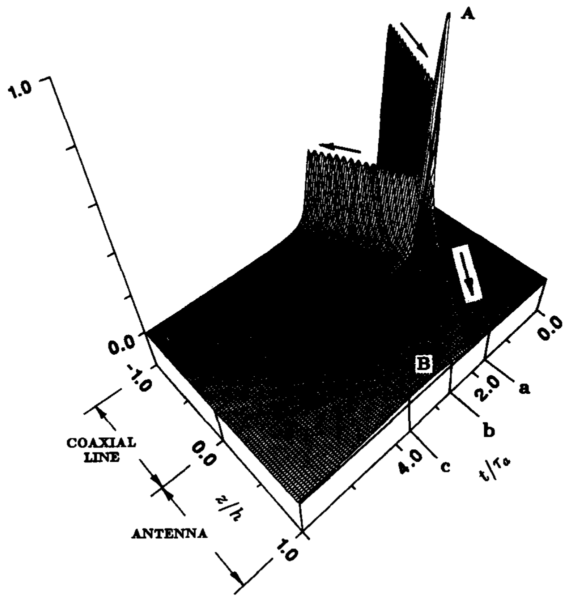

Fig. 2. Equivalent surface charge density on the resistive monopole antenna as a function of the normalized position z/h and the normalized time t/τ_a: Wu–King profile, $\psi_0 = 7.79$; $b/a = 2.30$, $h/a = 65.8$, and $\tau_p/\tau_a = 8.04 \times 10^{-2}$.

The high intensity of the electric field at the surface of the monopole (dark region on the gray scale plot, C in Fig. 3(c)) shows that significant charge remains on the monopole after the wavefront W_1 has been launched. This picture indicates that the charge density along the monopole increases away from the aperture. The lower charge density near the aperture is a result of rapid draining through the low resistance at this end of the monopole, while the higher charge density near the end is a result of slow draining through the entire resistance of the monopole.

The far-zone electric field, obtained by transforming the near-field results, is shown in Fig. 4(a). Each trace in this figure shows the electric field at a fixed polar angle, θ, as a function of the normalized time t/τ_a. The origin for the time, $t/\tau_a = 0$, and the amplitude of the field were selected to clarify the presentation. Notice that the radiated waveform at broadside ($\theta = 90°$) has an initial positive pulse, the wavefront W_1, which roughly resembles the Gaussian pulse excitation, followed by a long negative tail. The tail is partially due to the radiation that occurs when the wavefront W_1 moves along the monopole depositing charge. This tail is also clearly shown on the gray scale plot (T in parts (b) and (c) of Fig. 3). As the angle θ is decreased from 90°, the shape of the radiated waveform, particularly the long tail, changes. At angles near $\theta = 90°$, the times of arrival in the far zone for radiation produced at different points along the monopole are spread out.

---

[1] For the center conductor (perfectly conducting) the equivalent surface charge density is the actual surface charge density. However, for the tubular monopole (finite conductivity) the equivalent surface charge density is the total charge within the tube per unit area of the outer surface.

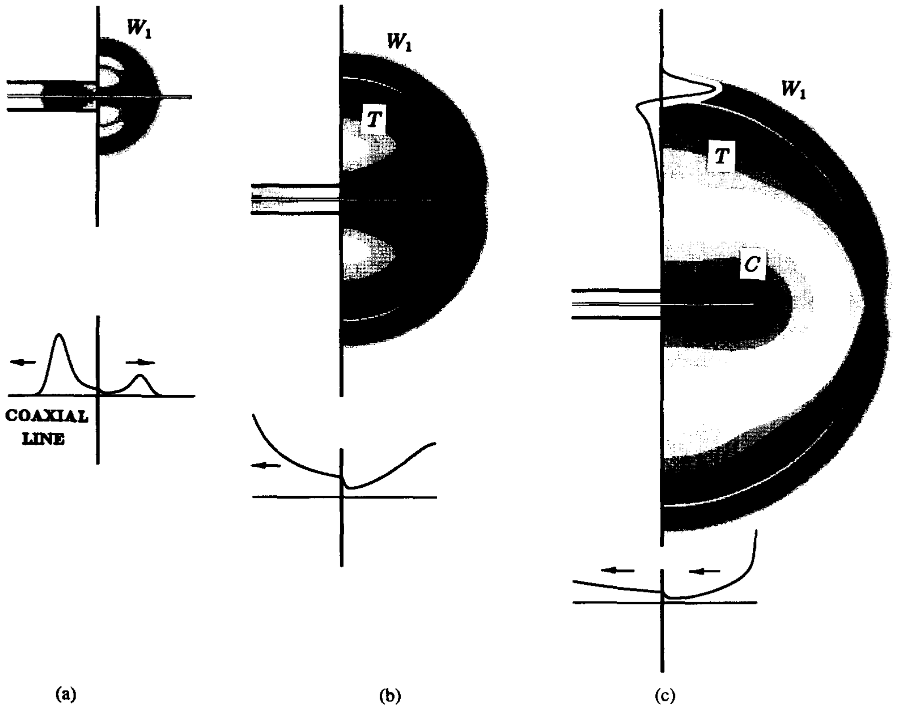

Fig. 3. Radiation of a Gaussian pulse from a resistive monopole antenna. Gray scale plots show the magnitude of the electric field; the line drawings below each plot show the equivalent surface charge density on the antenna. Wu-King profile, $\psi_0 = 7.79$; $b/a = 2.30$, $h/a = 65.8$, and $\tau_p/\tau_a = 8.04 \times 10^{-2}$. Charge density is scaled in (b) and (c) by a factor of 10.

Thus, the radiation associated with the deposition of charge along the monopole produces a tail roughly τ_a in length. At angles near $\theta = 0°$, the times of arrival in the far zone for radiation at different points along the monopole are the same. This leads to the compression of the tail to a length roughly equal to $2\tau_p$ ($\theta = 5°$ in Fig. 4(a)). A comparison of these results with those for the perfectly conducting monopole [1, fig. 7] shows that the resistive loading has eliminated the multiple wavefronts (W_2, W_3, $\cdots$ in [1, fig. 7]) associated with reflections at the end and coaxial aperture.

As a second example, the resistive monopole will be studied for a differentiated Gaussian excitation, the incident electric field being (7) with

$$\mathcal{V}^i(t) = -V_0(t/\tau_p)\exp(1/2 - t^2/2\tau_p^2). \qquad (9)$$

This pulse was chosen because it has zero mean (no dc component) and limited low-frequency content, in contrast to the Gaussian pulse, whose largest components are at low frequencies (significant dc component). A practical antenna of finite size cannot radiate the extremely low frequencies of the Gaussian pulse. Thus, for some applications the differentiated Gaussian pulse is a more realistic waveform to use in studying the distortion on radiation from a practical antenna.

Fig. 5 shows the electric field surrounding the resistive monopole, and Fig. 4(b) shows the far-zone electric field for excitation by the differentiated Gaussian pulse (9). All the parameters for the antenna and the pulse are the same as those used earlier for the Gaussian pulse excitation.

Notice that the charge deposited on the monopole (C in Fig. 5(c)) is much lower than it was with the Gaussian pulse (C in Fig. 3(c)). This is the result of the bipolar shape of the differentiated Gaussian waveform. As it moves out along the monopole, the positive charge deposited by the front of the waveform is partially canceled by the negative charge deposited by the back of the waveform. This causes a significant reduction in the long tail of the radiated waveform at broadside (compare (a) and (b) of Fig. 4 for $\theta = 90°$). Thus, this waveform more closely resembles the differentiated Gaussian excitation. However, there is still a significant change in the waveform as the angle θ is decreased toward 0°: at $\theta = 90°$ the waveform resembles the first derivative of the Gaussian, while at $\theta = 5°$ the waveform resembles the second derivative of the Gaussian.

A point of particular concern for resistive antennas is the decrease in the radiating efficiency caused by ohmic losses. The total energy radiated is easily computed by taking the time and surface integrals of the outward-pointing, normal component of the Poynting vector for a surface surrounding the monopole. In a similar manner, the total energies can be determined for the incident and reflected pulses in the coaxial line.

Table I shows the percentages of the energy in the incident pulse that are reflected in the coaxial line, radiated, and

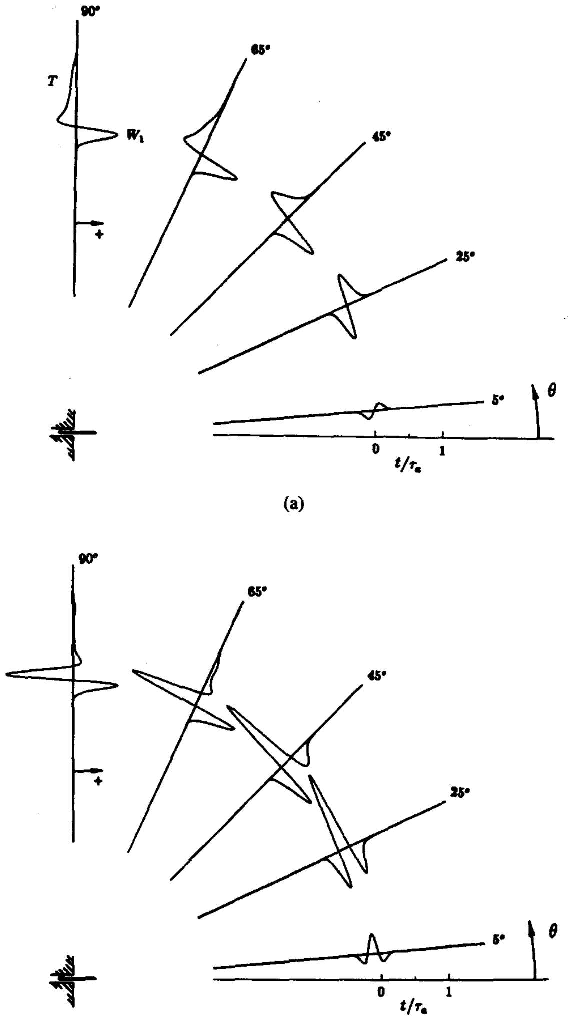

(a)

(b)

Fig. 4. Radiation of (a) a Gaussian pulse and (b) a differentiated Gaussian pulse from a resistive monopole antenna. Each trace shows the far-zone electric field $\mathcal{E}_\theta^r$ at a fixed polar angle θ as a function of the normalized time t/τ_a. Wu–King profile, $\psi_0 = 7.79$; $b/a = 2.30$, $h/a = 65.8$, and $\tau_p/\tau_a = 8.04 \times 10^{-2}$.

dissipated in the resistance of the monopole. Results are also given for a perfectly conducting monopole of the same geometry. Both Gaussian (8) and differentiated Gaussian (9) excitations are considered. The parameters for the monopole and excitation are the same as those used earlier.

For either method of excitation, the percentage of the incident energy reflected is roughly the same for both the resistive and perfectly conducting monopoles: 39% for the Gaussian, 21% for the differentiated Gaussian. Of course, the remainder of the incident energy is radiated from the perfectly conducting monopole: 61% for the Gaussian, 79% for the differentiated Gaussian. Whereas, for the resistive monopole only a portion of the remaining energy is radiated, 14% for the Gaussian and 23% for the differentiated Gaussian, the rest being dissipated in the structure. The radiating efficiency is

$$\frac{\text{energy radiated}}{\text{energy radiated} + \text{energy dissipated}}.$$

For the Gaussian excitation, the resistive monopole is 23% efficient, while for the differentiated Gaussian excitation it is 29% efficient. These values are consistent with those given by other investigators for antennas with Wu–King profiles operating at a single frequency [3], [4], [9], [16].

IV. DEVELOPMENT AND MEASUREMENT OF AN EXPERIMENTAL MODEL

The flexibility inherent in the FDTD method for handling fine geometrical and electrical details makes it possible to analyze a theoretical model that is essentially the same as a complex experimental model for an antenna. Thus it is reasonable to expect excellent agreement between theoretical and experimental results.

Various methods have been used to construct experimental models for resistive antennas with a Wu–King profile (3). These methods generally involve the deposition of a continuous resistive film of variable thickness on a dielectric rod [9], [11], [12], [16]. Often the difficulties encountered in accurately depositing the film have led to profiles that differed from (3).

Because of the difficulties and expense associated with constructing and characterizing a resistive profile made from a thin metallic film, it was decided to fabricate the experimental model from a set of discrete resistors. It was particularly important that the physical and electrical properties of these resistors be well known. Conventional resistors generally have electrical properties that change significantly in an unpredictable way as frequency is increased to the microwave range. Since the measurements to be reported here contain frequencies as high as 18 GHz, conventional resistors were unacceptable.

The commercially available, high-frequency resistors chosen for the experimental model have a dc resistance accurate to within 0.1% of the specified value. They are formed from a carbon film deposited on the surface of an alumina rod ($\epsilon_r \approx 10$), as shown in the inset on the right of Fig. 6. The geometrical and electrical details of these resistors can be included in the theoretical model and accurately analyzed by the FDTD method. In particular, the thin tubes of carbon film are efficiently handled by the new technique for treating thin-material sheets in the FDTD method [17]. In the analysis, each resistor is modeled by ten FDTD cells in length and one in radius; the thickness of the resistive film ($d \approx 1$ μm) is about 1/500th the width of a cell.

Fig. 7 shows the discretized version of the continuous Wu–King profile ($\psi_0 = 10.0$) used for the experimental model. It contains ten sections, each formed by soldering a group of resistors of equal value end to end. The average length of the 32 resistors used was $h_r = 3.57$ mm, making the total length of the monopole $h = 11.43$ cm. The other dimensions for the monopole and the coaxial feed line (APC-7) are $a = 1.52$ mm, $b = 3.50$ mm, $a_s = 1.59$ mm, $h_s = 6.88$ mm, and $a_m = a_r = 0.508$ mm. For the purpose of making this plot, the conductivity of the discretized profile over the length of

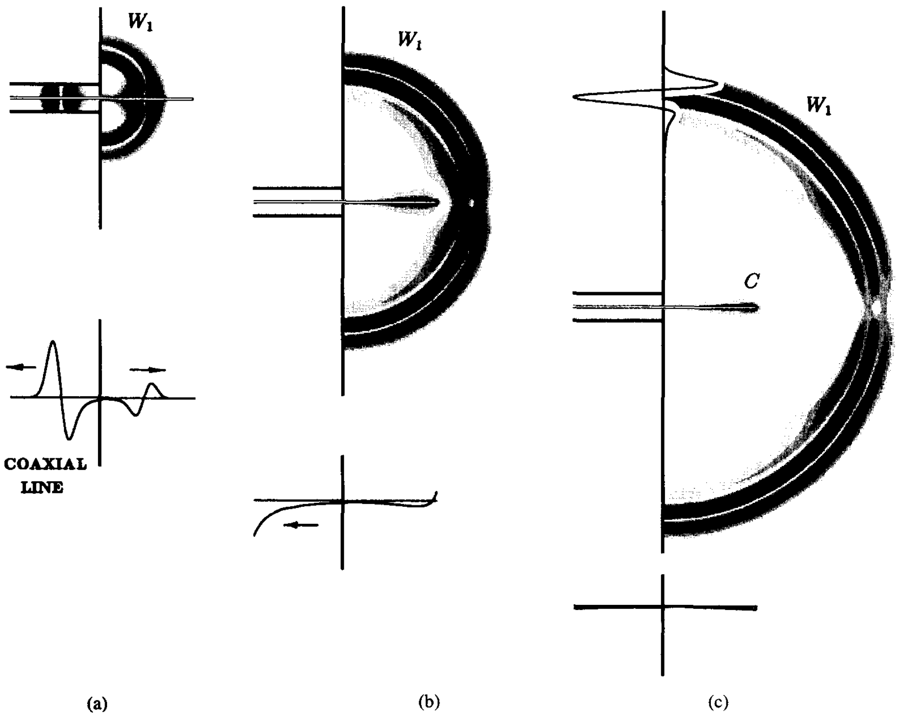

Fig. 5. Radiation of a differentiated Gaussian pulse from a resistive monopole antenna. Gray scale plots show the magnitude of the electric field; the line drawings below each plot show the equivalent surface charge density on the antenna. Wu–King profile, $\psi_0 = 7.79$; $b/a = 2.30$, $h/a = 65.8$, and $\tau_p/\tau_a = 8.04 \times 10^{-2}$. Charge density is scaled in (b) and (c) by a factor of 10.

TABLE I
ENERGY BUDGET FOR PERFECTLY CONDUCTING AND RESISTIVE MONOPOLES

Excitation Type	Antenna Structure	Percentage of Energy in Incident Pulse			Radiation Efficiency %
		Reflected	Radiated	Dissipated	
Gaussian	Perfectly Conducting	39	61	0	100
Gaussian	Resistive	38	14	48	23
Differentiated Gaussian	Perfectly Conducting	21	79	0	100
Differentiated Gaussian	Resistive	21	23	56	29

each section was calculated from the average resistance per unit length, $\bar{r}^i = R/h_r$, of the resistors in that section:

$$\sigma = 2\pi a_m d/\bar{r}^i. \tag{10}$$

In Fig. 8 the theoretical far-zone electric fields, $\mathcal{E}_\theta^r$, at broadside ($\theta = 90°$) for monopoles with the continuous (solid line) and discretized (dash line) profiles are compared. The excitation is a Gaussian pulse (8) with $\tau_p/\tau_a = 7.04 \times 10^{-2}$. Notice that the discretization of the profile produces only a small change along the tail of the pulse.

The experimental model was mounted on an aluminum image plane (120 cm × 155 cm) that was surrounded by absorbing material to reduce reflections. A small monopole probe ($h_{probe} \approx 6$ mm) was mounted on the image plane at the radial distance $r_{probe} = 63.5$ cm from the antenna under test. The input reflection coefficient for the antenna (S_{11}) and the transmission coefficient (S_{21}) between the antenna and monopole probe were measured at a number of frequencies (45 MHz $\leq f \leq$ 18.045 GHz) using a Hewlett-Packard model 8510 automated network analyzer. These data were then used with a fast Fourier transform to obtain the response of the antenna to a Gaussian pulse (8). An experimentally determined transfer function was used to remove the frequency dependence on reception of the small monopole probe [20].

In Fig. 9 the reflected voltage measured in the coaxial line (dots) is compared with the results computed by the FDTD method (solid line) for a unit amplitude, Gaussian pulse excitation with $\tau_p/\tau_a = 7.04 \times 10^{-2}$. Fig. 9(a) is for the monopole with the Wu–King profile, and Fig. 9(b) is for a roughly equivalent metallic monopole ($h = 11.44$

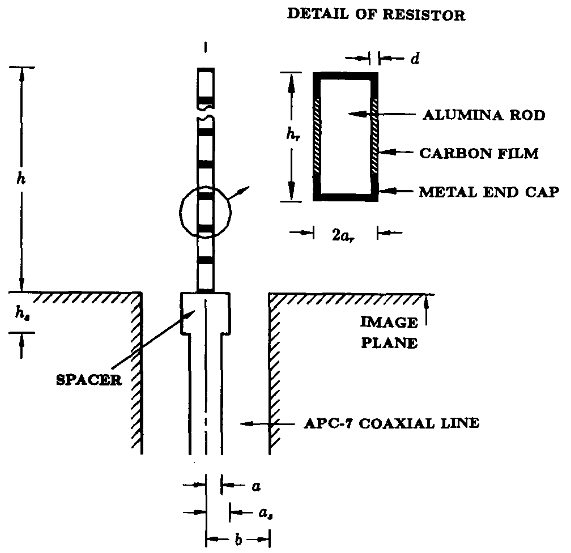

Fig. 6. Experimental model for resistive monopole antenna fed through an image plane by a coaxial line. Note detail of individual resistors.

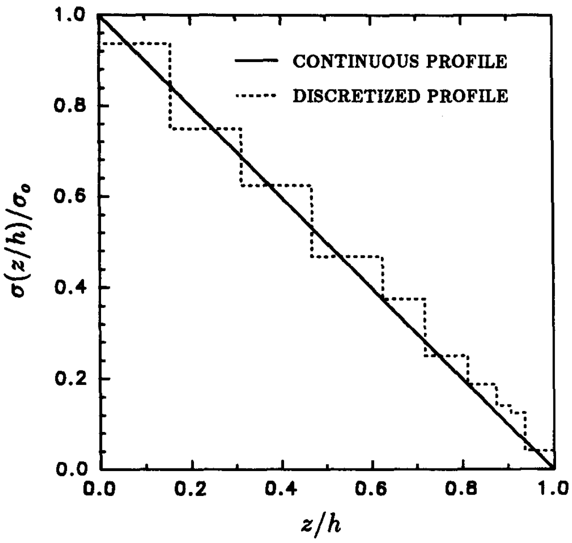

Fig. 7. Discretization of continuous profile used with experimental model.

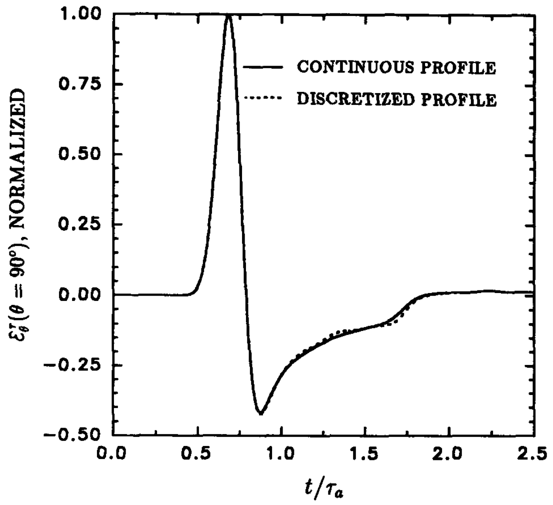

Fig. 8. Comparison of far-zone radiated waveforms, $\mathcal{E}_\theta^r(\theta = 90^\circ)$, for monopoles with continuous and discretized Wu–King profiles, $\psi_0 = 10.0$; $b/a = 2.30$, $h/a_m = 225.0$, and $a_m/a = 0.334$. FDTD results for a Gaussian pulse excitation, $\tau_p/\tau_a = 7.04 \times 10^{-2}$.

cm, $a_m = 0.460$ mm). Notice that the early-time record ($t/\tau_a \leq 2.5$) has been expanded on these graphs. These results clearly show that both the resistive and the metallic monopoles have significant reflections at the drive point ($t/\tau_a \approx 0$), with the peak reflected amplitude being approximately 0.6 of the peak incident amplitude. For the resistive monopole there are no additional distinct reflections; however, there is a long tail on the waveform. For the metallic monopole there are several distinct reflections spaced by about the round-trip transit time for the pulse on the antenna, $t/\tau_a = 2.0$. The agreement between the measured and the FDTD results is excellent for both antennas.

Fig. 10 shows the electric field component $\mathcal{E}_\theta$ measured with the small monopole probe ($\tau_p/\tau_{probe} = c\tau_p/h_{probe} = 1.34$) at the distance $r_{probe}/h = 5.56$. Results are shown for the resistive monopole, Fig. 10(a), and the metallic monopole, Fig. 10(b). Again, the measured results (dots) are compared with the FDTD results (solid line). The units for the amplitude in both graphs are the same, and the early time record ($t/\tau_a \leq 6.5$) has been expanded. The radiation from the resistive monopole is a single waveform (initial pulse followed by a tail), while the radiation from the metallic monopole contains several elements, each associated with a reflection at the drive point or end of the antenna. Again, the agreement between measured and FDTD results is excellent for both antennas. Any small differences between the theoretical and experimental results are thought to be due to imperfections in the construction of the experimental model, e.g., slight tilt to the antennas or small bumps of solder at resistor junctions.

V. CONCLUSION

The resistively loaded monopole antenna with a Wu–King profile was considered as a radiator of temporally short, broadband pulses. Theoretical calculations made with the FDTD method were used to describe the radiation from this antenna in space and time. Specifically, graphical displays of these results were used to provide new insight into the physical processes for transient radiation from this antenna.

An experimental model was fabricated with a discretized version of the Wu–King profile that was constructed from a set of precision resistors. The geometrical and electrical parameters for the resistors were precisely known and included in the corresponding theoretical model and FDTD analysis. Measurements of both the reflected voltage in the feed line and the time-varying radiated field from this antenna were in excellent agreement with the theoretical calculations. A survey

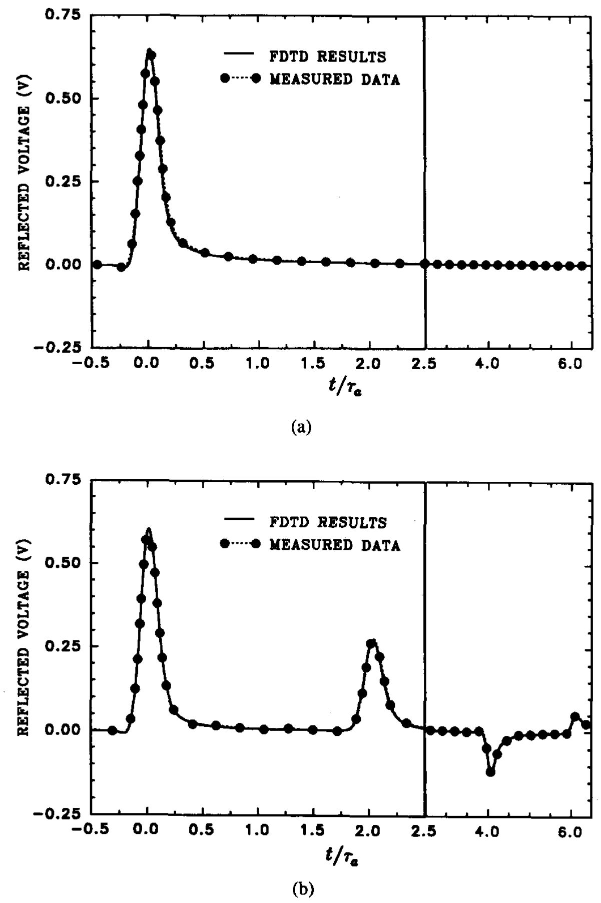

(a)

(b)

Fig. 9. Comparison of the FDTD theoretical and the measured reflected voltages in the coaxial line for a cylindrical monopole antenna excited by a 1 V Gaussian pulse, $\tau_p/\tau_a = 7.04 \times 10^{-2}$, $b/a = 2.30$. (a) Wu-King monopole, $\psi_0 = 10.0, a_m/a = 0.334, h/a_m = 225$; (b) metallic monopole, $a_m/a = 0.303$, $h/a_m = 249$.

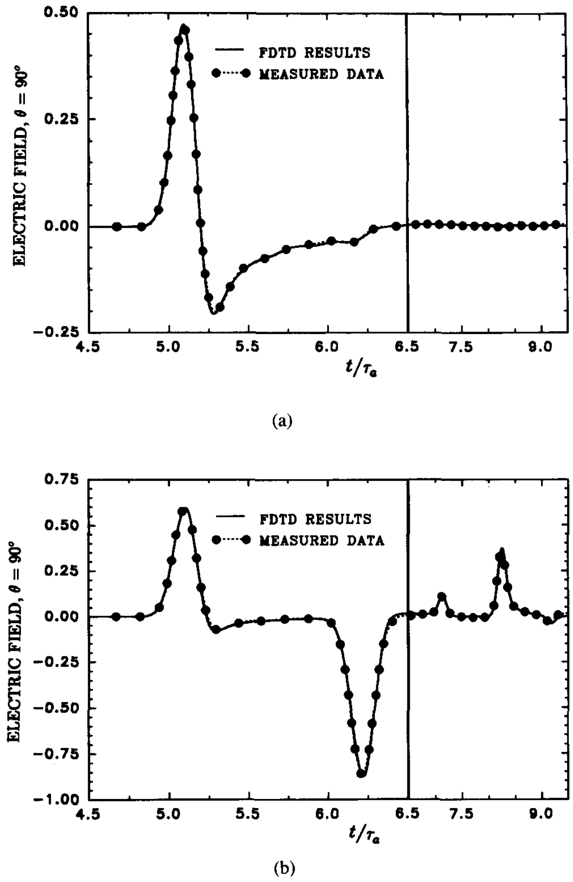

(a)

(b)

Fig. 10. Comparison of the FDTD theoretical and the measured radiated waveforms at broadside for a cylindrical monopole antenna excited by a 1 V Gaussian pulse, $\tau_p/\tau_a = 7.04 \times 10^{-2}$, $b/a = 2.30, r_{\text{probe}}/h = 5.56$. (a) Wu-King monopole, $\psi_0 = 10.0, a_m/a = 0.334, h/a_m = 225$; (b) metallic monopole, $a_m/a = 0.303$, $h/a_m = 249$.

of the literature for this antenna shows that no better agreement has been obtained. This is the first time that the radiated fields of antennas computed by the FDTD method have been compared with measured results in the time domain; this was not done in the previous paper [1].

REFERENCES

[1] J. G. Maloney, G. S. Smith, and W. R. Scott, Jr., "Accurate computation of the radiation from simple antennas using the finite-difference time-domain method," *IEEE Trans. Antennas Propagat.*, vol. 38, pp. 1059–1068, July 1990.

[2] E. E. Altshuler, "The traveling-wave linear antenna," *IRE Trans. Antennas Propagat.*, vol. 9, pp. 324–329, July 1961.

[3] T. T. Wu and R. W. P. King, "The cylindrical antenna with nonreflecting resistive loading," *IEEE Trans. Antennas Propagat.*, vol. 13, pp. 369–373, May 1965. Correction, p. 998, Nov. 1965.

[4] L.-C. Shen and T. T. Wu, "Cylindrical antenna with tapered resistive loading," *Radio Sci.*, vol. 2, pp. 191-201, Feb. 1967.

[5] C. D. Taylor, "Cylindrical transmitting antenna: Tapered resistivity and multiple impedance loadings," *IEEE Trans. Antennas Propagat.*, vol. 16, pp. 176–179, Mar. 1968.

[6] Y. P. Liu and D. L. Sengupta, "Transient radiation from a linear antenna with nonreflecting resistive loading," *IEEE Trans. Antennas Propagat.*, vol. 22, pp. 212–220, Mar. 1974.

[7] D. L. Sengupta and Y. P. Liu, "Analytical investigation of waveforms radiated by a resistively loaded linear antenna excited by a Gaussian pulse," *Radio Sci.*, vol. 9, pp. 621–630, June 1974.

[8] G. C. Rose and R. S. Vickers, "Transient response of resistively loaded cylindrical antennas," *Int. J. Electronics*, vol. 36, no. 4, pp. 479–486, 1974.

[9] M. Kanda, "A relatively short cylindrical broadband antenna with tapered resistive loading for picosecond pulse measurements," *IEEE Trans. Antennas Propagat.*, vol. 26, pp. 439–447, May 1978.

[10] F. W. Kappen and G. Mönich, "Single pulse radiating from a resistive coated dipole-antenna," in *Proc. Fifth Int. Conf. Antennas and Propagation (ICAP 87)* Mar. 1987, pp. 90–93.

[11] L. C. Shen, "An experimental study of the antenna with nonreflecting resistive loading," *IEEE Trans. Antennas Propagat.*, vol. 15, pp. 606–611, Sept. 1967.

[12] J. F. Lally and D. T. Rouch, "Experimental investigation of the broadband properties of a continuously loaded resistive monopole," *IEEE Trans. Antennas Propagat.*, vol. 18, pp. 764–768, Nov. 1970.

[13] M. Kanda and L. D. Driver, "An isotropic electric-field probe with tapered resistive dipoles for broad-band use, 100 kHz to 18 GHz," *IEEE Trans. Microwave Theory Tech.*, vol. 35, pp. 124–130, Feb. 1987.

[14] K. P. Esselle and S. S. Stuchly, "Pulse-receiving characteristics of resistively loaded dipole antennas," *IEEE Trans. Antennas Propagat.*, vol. 38, pp. 1677–1683, Oct. 1990.

[15] K. P. Esselle and S. S. Stuchly, "A broad-band resistively loaded V-antenna: Experimental results," *IEEE Trans. Antennas Propagat.*, vol. 39, pp. 1587–1591, Nov. 1991.

[16] B. R. Rao, "Optimized tapered resistivity profiles for wideband HF

monopole antenna," in *Proc. 1991 IEEE Antennas and Propagation Symp. Dig.*, (London, Ontario, Canada), vol. 2, June 1991, pp. 711–714.

[17] J. G. Maloney and G. S. Smith, "The efficient modeling of thin material sheets in the finite-difference time-domain (FDTD) method," *IEEE Trans. Antennas Propagat.*, vol. 40, pp. 323–330, Mar. 1992.

[18] A. Taflove, "Review of the formulation and applications of the finite-difference time-domain method for numerical modeling of electromagnetic wave interactions with arbitrary structures," *Wave Motion*, vol. 10, pp. 547–582, 1988.

[19] K. S. Yee, D. Ingham, and K. Shlager, "Time-domain extrapolation to the far field based on FDTD calculations," *IEEE Trans. Antennas Propagat.*, vol. 39, pp. 410–413, Mar. 1991.

[20] J. G. Maloney, "Analysis and synthesis of transient antennas using the finite-difference time-domain (FDTD) method," Ph.D. dissertation, Georgia Institute of Technology, Nov. 1992.

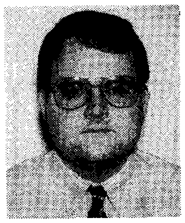

James G. Maloney (S'85–M'92) was born in New York, NY, on August 17, 1965. He received the B.E.E. and Ph.D. degrees from the Georgia Institute of Technology, Atlanta, GA, in 1987 and 1992, respectively.

From 1987 to 1989, he was a Graduate Research and Teaching Assistant in the School of Electrical Engineering at the Georgia Institute of Technology, and from 1989 to 1992, he was a J.S.E.P. Fellow at the Georgia Institute of Technology. Currently, he is a Research Engineer in the Signature Technology Lab at the Georgia Tech Research Institute.

Glenn S. Smith (S'65–M'72–SM'80–F'86) was born in Salem, MA, on June 1, 1945. He received the B.S.E.E. degree from Tufts University, Medford, MA, in 1967 and the S.M. and Ph.D. degrees in applied physics from Harvard University, Cambridge, MA, in 1968 and 1972, respectively.

From 1972 to 1975 he served as a Postdoctoral Research Fellow at Harvard University and also as a part-time Research Associate and Instructor at Northeastern University, Boston, MA. In 1975, he joined the faculty of the Georgia Institute of Technology, Atlanta, GA, where he is currently Regents' Professor of Electrical Engineering.

Dr. Smith is coauthor of the book *Antennas in Matter: Fundamentals, Theory and Applications*.